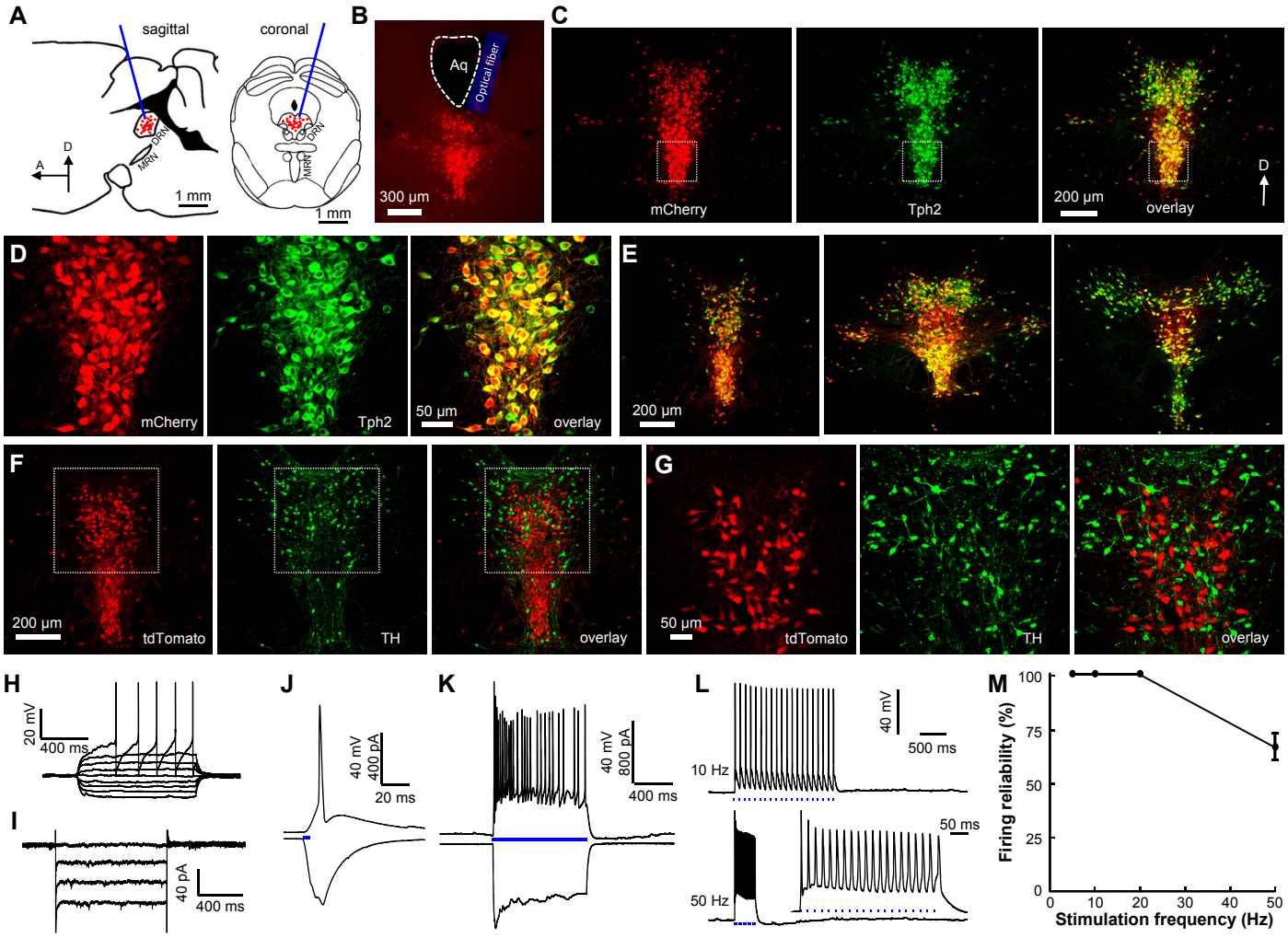

Figure S1. ePet1-Cre drives gene expression in 5-HT neurons and enables precise optogenetic activation. Related to Figure 1. (**A**) Diagrams illustrating the angles and tip location of virus-injecting cannulae and optical fibers. (**B**) A picture showing ChR2-mCherry expression in the DRN. The overlaying placement of an optical fiber was based on the lesion track. Aq, aqueduct. (**C** and **D**) In ePet1-Cre mice, infusion of AAV-DIO-mCherry virus resulted in expression of mCherry (red) in Tph2-immunopositive neurons (green) in the DRN. Panels in (D) show zoom-in views of the dashed area in (C). (**E**) Three coronal sections showing that Pet-1^{+} neurons were efficiently labeled in the anterior (left), middle, and posterior (right) parts of the DRN. The level of mCherry expression tended to be lower in the two lateral wings. Red, mCherry; green, Tph2 immunoreactivity. (**F** and **G**) Pet-1 neurons are not dopaminergic. Pet-1 neurons were labeled by crossing the ePet1-Cre mouse line with the Ai14 reporter line. None of the tdTomato+ Pet-1 neurons were immunopositive to tyrosine hydroxylase (TH), a marker of dopamine neurons. (**H** and **I**) Traces from current-clamp recordings (H) and voltage-clamp recordings (I) show the intrinsic properties of a ChR2-mCherry^{+} neuron in the DRN. Current injections ranged from -40 to 40 pA with a 10 pA interval (H) and voltage commands were applied at 5 mV per step (I). (**J**) Single brief light pulses (5 ms) elicited a large depolarizing potential and the firing of an action potential in the current-clamp mode (upper) and a strong inward current in the voltage-clamp mode (lower). (**K**) Sustained light pulses (1 s) resulted in depolarization and action potential firing in the current-clamp mode (upper) and a strong inward current in the voltage-clamp mode (lower). (**L**) Trains of brief light pulses (blue dots) produced temporally precise firing of action potentials at the frequency of 10 and 50 Hz. Inset shows the zoom-in view of the spiking activity in response to 50 Hz stimulation. (**M**) The mean ratio of successful spike generation in relationship to light stimulation at different frequencies (n = 8 cells). Error bars indicate SEM in this and following figures.

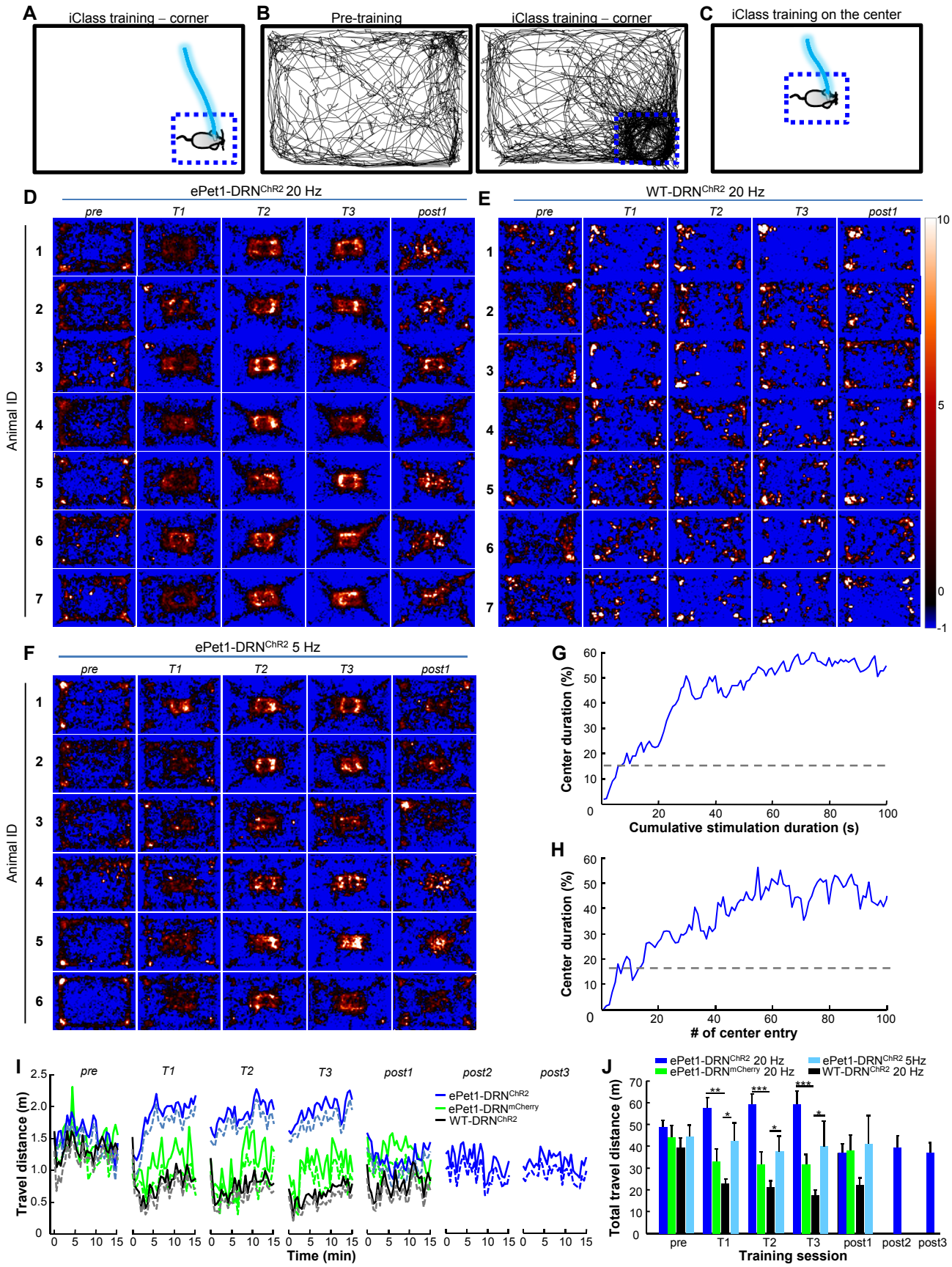

Fig S2; Supplemental Online Material page 2

Figure S2. Coupling light stimulation with animal navigation in a specific subarea reinforces exploration within the stimulation-coupled area. Related to Figure 1. (**A**) The method of iClass training by coupling light stimulation to animal exploration in a corner (dashed blue box). (**B**) When DRN stimulation was coupled to the entry of the ePet1-DRN^{ChR2} mouse to the lower right corner (the dashed blue box), the animal explored the stimulated corner much more intensively. (**C**) The method of iClass training by coupling light stimulation to animal exploration in the center of an open field. (**D)** Heat maps showing the spatial distribution of exploration time before (*pre*), during (*T1-3*) and after (*post*) iClass trainings on ePet1-DRN^{ChR2} mice (n = 7). The color scale at the right indicates the fold differences between actual time and the time normalized by the total area of the open field, with red indicating higher level of exploration than average (preference) and blue indicating lower levels (avoidance). (**E**) The iClass training did not have any effect on control animals, which were nontransgenic animals with AAV-DIO-ChR2-mCherry vector injection into the DRN (n = 7 WT-DRN^{ChR2} mice). (**F**) Heat maps showing that the iClass training with 5 Hz stimulation increased the duration of central exploration (n = 6 ePet1-DRN^{ChR2} mice). Dashed lines indicate mean - SEM. (**G**) The relationship between the instantaneous ratio of center duration (vertical axis) and the cumulative DRN-stimulation duration (horizontal axis) in the T1 session of ePet1-DRN^{ChR2} mice (n = 7). The dashed horizontal line represents the value of mean + 3SEM calculated from the baseline of pre-training sessions and corresponds to a p value of 0.001. (**H**) Plot of the instantaneous time ratio in relationship to the cumulative center entries. (**I**) The instantaneous travel distance for ePet1-DRN^{ChR2} mice (blue, n = 7), WT-DRN^{ChR2} mice (black, n = 7), and ePet1-DRN^{mCherry} mice (green, n = 5). (**J**) Bar plot shows significantly longer travel distance of ePet1-DRN^{ChR2} mice during the iClass training sessions (*, $p<0.05$; **, $p < 0.01$; ***, $p<0.001$; Tukey's multiple comparisons test between animal groups after two-way ANOVA).

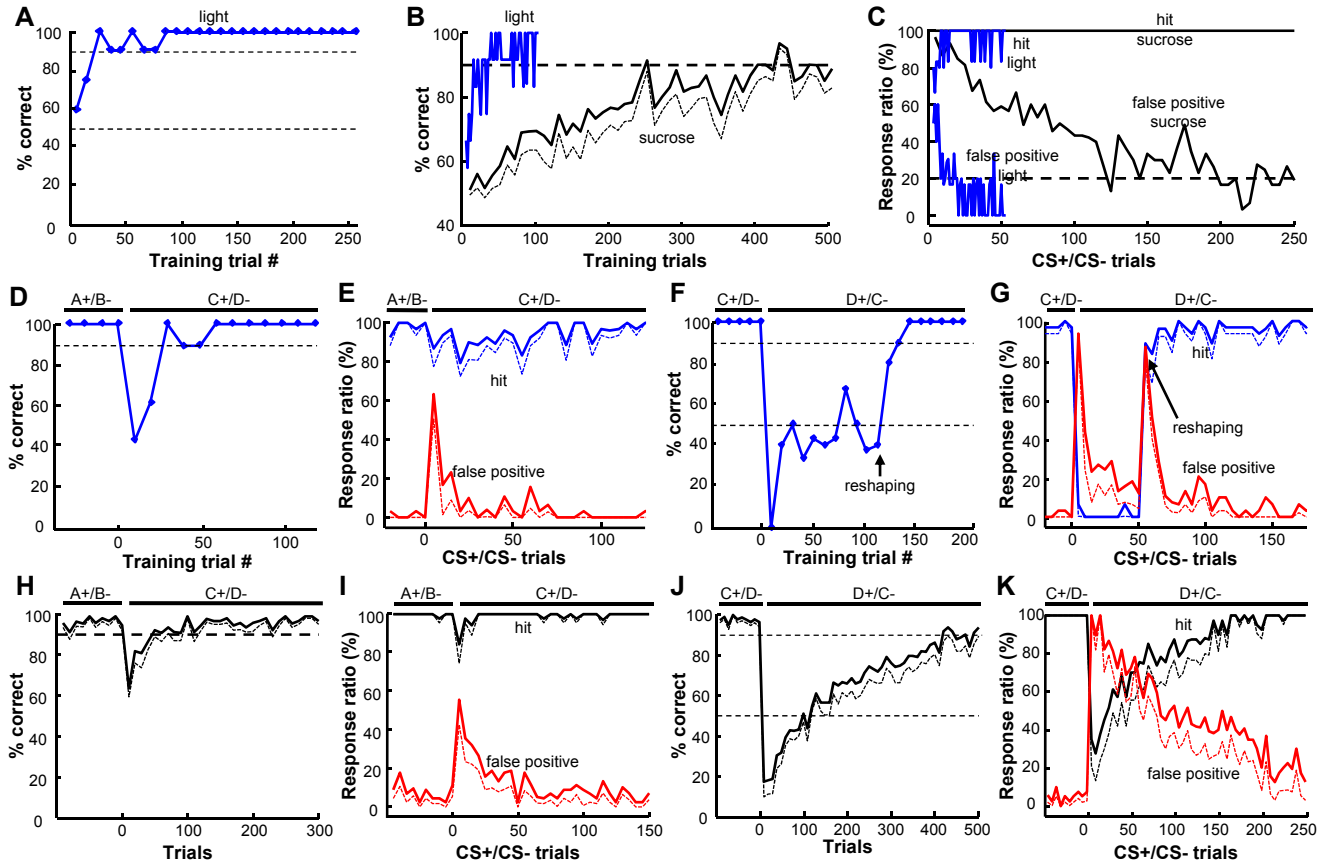

Figure S3. Detailed analyses of olfactory discrimination learning guided by DRN light stimulation or sucrose rewards. Related to Figure 3. (**A**) The learning curve of an ePet1-DRN^{ChR2} mouse trained with DRN light stimulation. (**B**) Mean learning curves of the initial 500 trials for mice trained with sucrose solution and the initial 100 trials for mice trained with light stimulation. Dashed lines indicate mean - SEM. Each point represents 10 trials averaged across individual mice trained with sucrose solution and 2 trials for mice with light stimulation. (**C**) The ratio of hit responses to CS+ odor and that of false positive responses to CS- odor. Each trial block contains CS+ and CS- stimuli that were presented in a pseudorandom order. A total of 500 trials consisted of 250 CS+ trials and 250 CS- trials. (**D** and **E**) Learning curve of an ePet1-DRN^{ChR2} mouse (D) and the plot of mean response ratio for all test mice (E) after the original conditioning odors (odor A as CS+ and B as CS-; A+/B-) were switched to a novel pair of conditioning odors (odor C as CS+ and D as CS-; C+/D-). These mice were trained with DRN light stimulation (n = 6 mice). (**F** and **G**) The mean learning curve and the ratios of hit and false positive responses of ePet1-DRN^{ChR2} mice challenged with valence reversal of conditioning odor stimuli (from C+/D- to D+/C-). During the initial 20 trials of the reversal (10 CS+ or CS- trials in panel G), mice continued to respond to the now CS- and failed to respond to the now CS+, resulting in 50% correct ratio. Then mice abandoned licking following either CS+ or CS-. After reshaping, mice licked in response to both CS+ and CS- and then rapidly reduced their false positive responses to CS-. (**H-K**) The performance of wild-type mice with the reward of sucrose solution for the tests of odor switch (H and I) and reversal (J and K). n =9 mice.

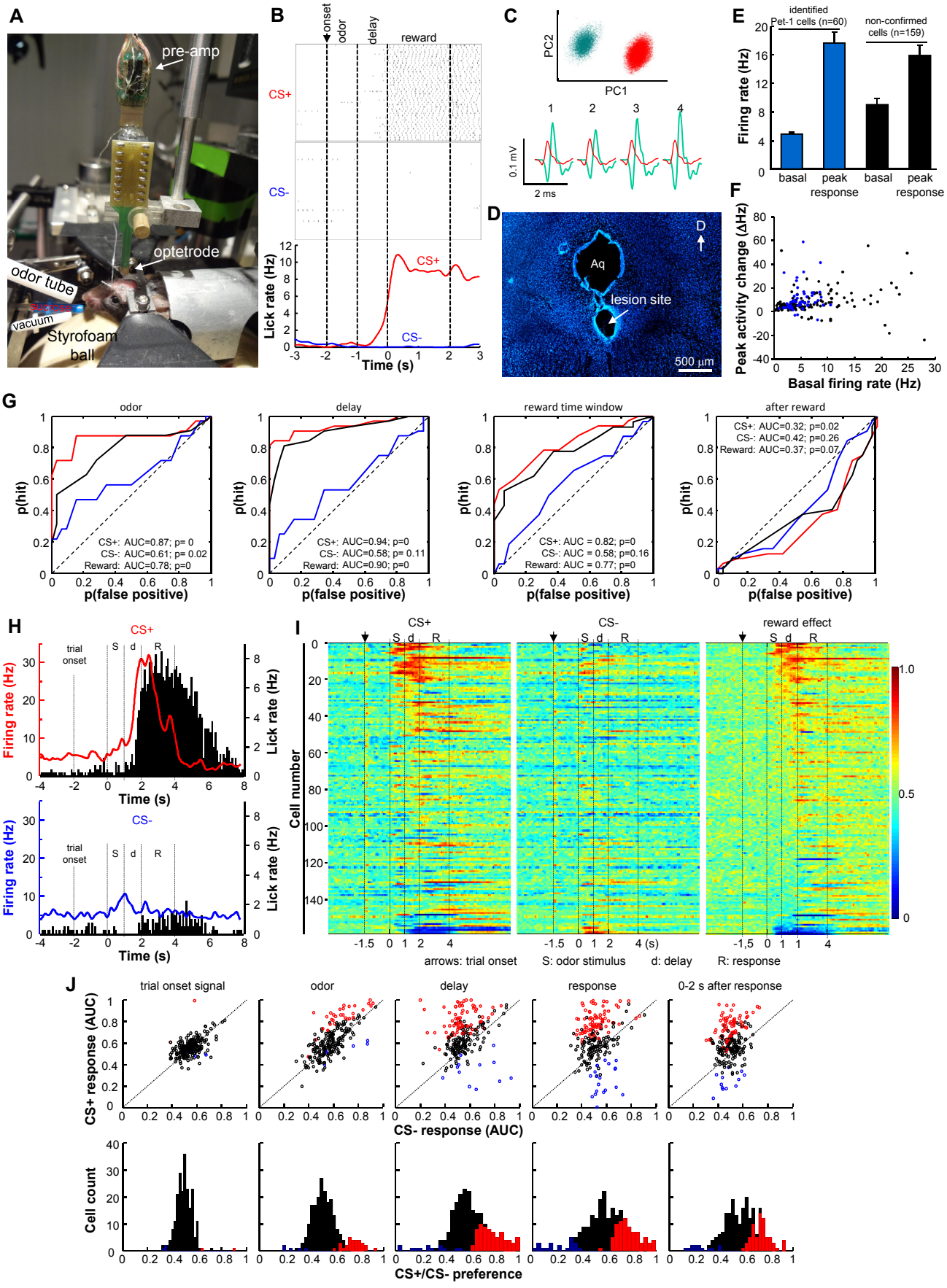

Fig S4; Supplemental Online Material page 5

Figure S4. Tetrode recordings from the DRN of mice engaged in an olfactory discrimination task. Related to Figure 4. (**A**) A picture showing the method of tetrode recording from head-fixed behaving mice. A mouse was placed on a spherical treadmill and accessed sucrose solution following one specific odor (CS+, 1s). (**B**) After training with the Go/No-go paradigm, mice responded with licking for sucrose consumption only after the reward-positive odorant (CS+, top panel) but not the reward-negative odorant (CS-, middle panel). The bottom panel shows the mean instantaneous lick rates during CS+ trials (red) and CS- trials (blue), respectively. The dashed lines indicate the time lines for trial onset, odor delivery, delay, and response time window for licking. (**C**) The methods of spike sorting. Spiking signals were recorded and single units were sorted using the Spike2 software for tetrode recordings. This program utilizes principle component analysis (PCA, upper panel) and takes advantage of the fact that spikes from the same single cell often appear simultaneously on the four recording points of the same tetrode with slightly different spike waveforms. In this example, two different single units (green and red) were sorted out from one tetrode. Numbers 1-4 indicate 4 recording sites of a tetrode. (**D**) After recordings, electrolytic lesion was made to confirm that the recording site was located within the DRN. Blue indicates DAPI counterstaining of cell nuclei. Aq: aqueduct. (**E**) The basal firing rates and peak firing rates of optogenetically confirmed DRN Pet-1 neurons (n=60) as well as DRN cells that were not confirmed with the method of optical tagging (n=159). (**F**) Distribution of basal firing rates and peak firing rates to CS+ of all recorded DRN neurons. Blue dots indicate positively identified Pet-1 neurons. Black dots indicate randomly recorded DRN cells. (**G**) ROC curves of a Pet-1 cell for CS+, CS- and net reward effects during different phases of the olfactory discrimination task. (**H**) Plots of PSTH of a randomly recorded DRN neuron (smoothed lines) and licking events (histogram) of the mouse for CS+ (upper) and CS- (lower) trials. PSTH bin = 100 ms. (**I**) Heat maps showing the response patterns of 159 DRN cells that were not identified with optetrodes. Although many of these cells were also selectively activated during reward-associated tasks, a more diverse response pattern was observed. Many cells were briefly activated during the onset of both CS+ and CS- trials. Some cells were inhibited by CS+ odors. Color scale at right indicates response intensity for the CS+ and CS- maps (left and middle panels) and CS+/CS- selectivity for the reward effect map (right panel), with a value of 0.5 indicates no response or no selectivity. (**J**) The distribution of neuronal response selectivity to CS+ and CS- trials during different task phase (trial onset, odor, delay, response, after response). Upper panels show the scatter plots of neuronal response strength as ROC values to CS+ and CS- trials. Each dot indicates one neuron. Lower panels plot the distribution of neuronal response selectivity to CS+ or CS- during each epoch. Response selectivity was calculated as ROC values. Neurons with significant selectivity for CS+ trials are shown in red and those with significant selectivity for CS- trials in blue (permutation test, $p < 0.01$). .

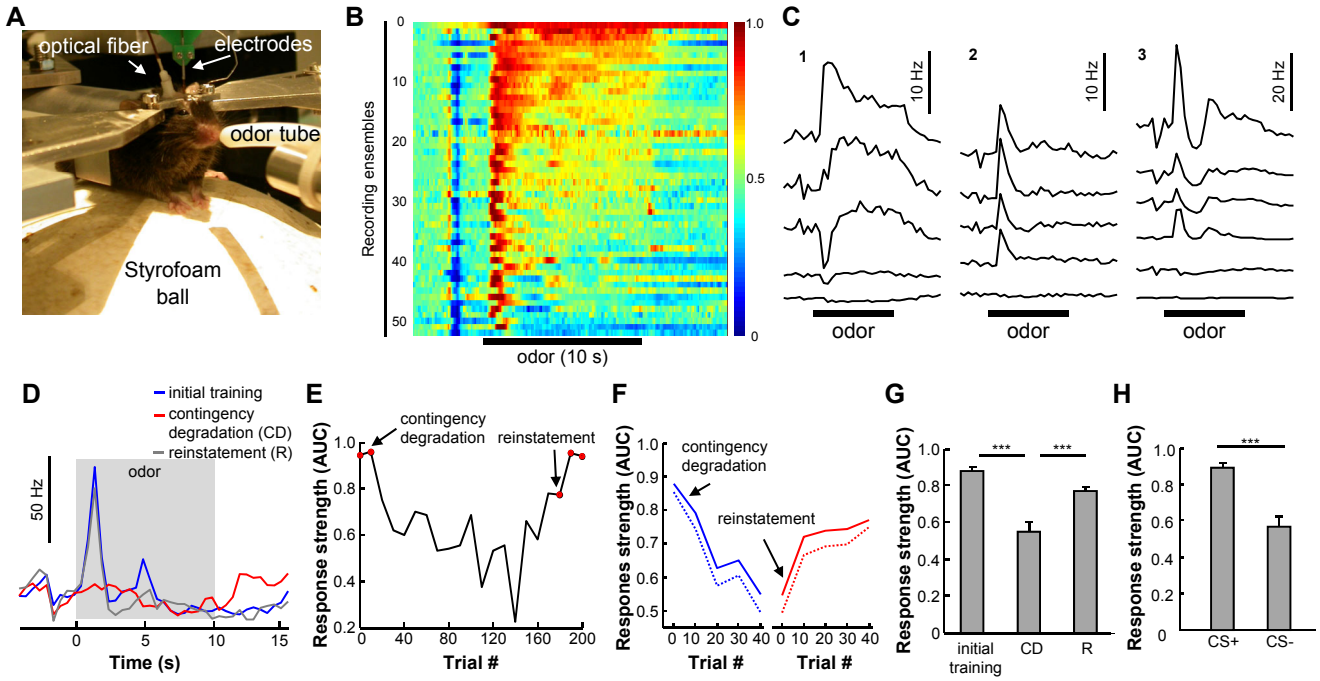

Figure S5. Optogenetic stimulation of DRN Pet-1 neurons guides rapid neuroprosthesis learning at the level of single neurons. Related to Figure 5. (**A**) A picture showing the setup for recording and optogenetic stimulation of a head-fixed behaving mouse on a spherical treadmill. Optical fiber was implanted over the DRN and electrodes consisting of 4 tetrodes were targeted at the vM1 cortical area. (**B**) A heat map showing that ensemble firing activity increased in response to odorant application after training (n = 52 recording sites). (**C**) Data from three representative recording sites illustrate that cortical neurons often exhibited different response patterns. Some single neurons within a recording site showed strong excitation, whereas others responded more mildly or did not respond at all. Some cells showed tonic activation (left), but others responded with phasic excitation at the onset of odorant application (middle). In additions, some cells responded with more complex patterns of multiple excitation peaks (right). (**D**) After training, odor-evoked responses of an ensemble were drastically reduced when the contingency between odor pulses and laser stimulation was degraded. Performance returned to pre-degradation level after the coupling between laser and odor-evoked responses was reinstated. Data from single trials were plotted. (**E**) Time-series plot of the response strength, showing the effect of contingency degradation and stimulation reinstatement. Red dots indicate significant responses ($p<0.01$; permutation test). AUC, the area under a ROC curve. (**F**) Population data showing the effects of contingency degradation and reinstatement across time (n = 12 ensembles from 5 mice). (**G**) Group data of contingency degradation tests (***, $p < 0.001$; paired t-test). (**H**) The learning guided by DRN stimulation is odor-specific. After successful training with citral only, citral and ethanol were given in a pseudo-random order. Ethanol were not coupled to light and produced significantly lower level of correct responses (**, $p < 0.01$; paired t-test; n = 10 ensembles from 4 mice).

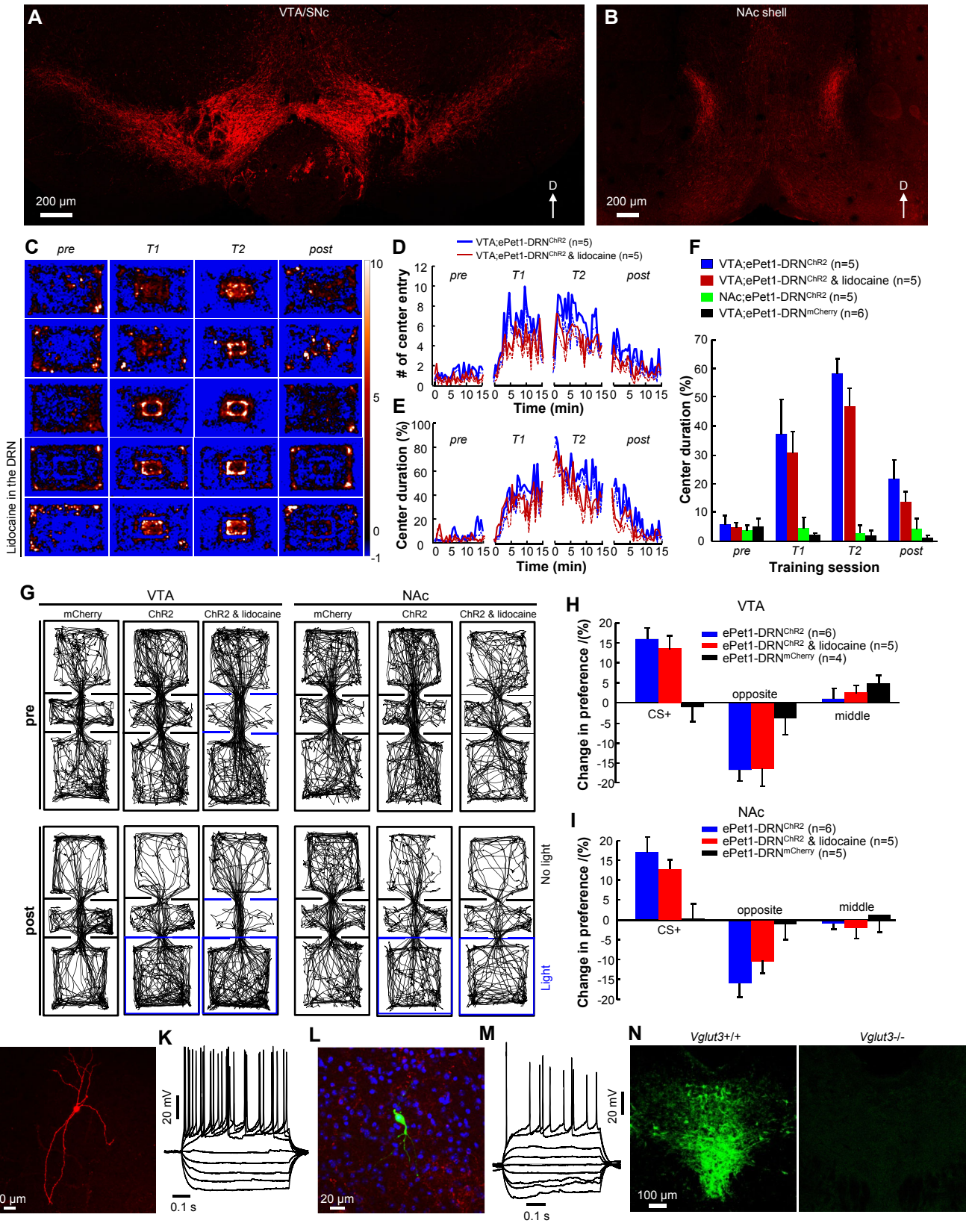
A
VTA/SNc
200 µm
D
B
NAc shell
200 µm
D
C
pre
T1
T2
post
Lidocaine in the DRN
10
5
0
-1
D
VTA;ePet1-DRNChR2 (n=5)
VTA;ePet1-DRNChR2 & lidocaine (n=5)
# of center entry
Time (min)
E
Center duration (%)
Time (min)
F
VTA;ePet1-DRNChR2 (n=5)
VTA;ePet1-DRNChR2 & lidocaine (n=5)
NAc;ePet1-DRNChR2 (n=5)
VTA;ePet1-DRNmCherry (n=6)
Center duration (%)
Training session
G
VTA
NAc
mCherry
ChR2
ChR2 & lidocaine
pre
post
No light
Light
H
VTA
ePet1-DRNChR2 (n=6)
ePet1-DRNChR2 & lidocaine (n=5)
ePet1-DRNmCherry (n=4)
Change in preference /(%)
CS+
opposite
middle
I
NAc
ePet1-DRNChR2 (n=6)
ePet1-DRNChR2 & lidocaine (n=5)
ePet1-DRNmCherry (n=5)
Change in preference /(%)
CS+
opposite
middle
J
20 µm
K
20 mV
0.1 s
L
20 µm
M
20 mV
0.1 s
N
Vglut3+/+
Vglut3-/-
100 µm

Figure S6. Stimulating axonal terminals of DRN Pet-1 neurons in the VTA and the NAc produces reward. Related to Figure 6. **(A and B)** ChR2-mCherry labeling shows that DRN Pet-1 neurons project their axons heavily to the VTA/SNc (A) and the NAc shell (B) in an ePet1-DRN^{ChR2} mouse. (**C**) Stimulating axonal terminals of DRN Pet-1 neurons in the midbrain VTA increased animal exploration in the center of open fields for all ePet1-DRN^{ChR2} test mice. The upper three rows show the heat maps of three out of the five test animals. The lower two rows are the heat maps of two out of another five mice that were given lidocaine in the DRN immediately before terminal stimulation in the VTA. (**D** and **E**) Plots of the number of center entries (D) and the instantaneous center duration (E) of ePet1-DRN^{ChR2} mice across different iClass sessions, with or without prior lidocaine injection into the DRN. *pre*, pre-training session; *T1* and *T2*, iClass training sessions 1 and 2; *post*, extinction session. (**F**) Group data show that stimulating axon terminals in the VTA but not the NAc reinforced center exploration of ePet1-DRN^{ChR2} mice. VTA stimulation in ePet1-DRN^{mCherry} mice was used as a control. (**G-I**) Stimulating axonal terminals of DRN Pet-1 neurons in the midbrain VTA or in the NAc causes conditioned place preference. (**G**) Locomotion tracks show that stimulation of axonal terminals in the VTA or the NAc of ePet1-DRN^{ChR2} mice enhanced exploration in the chamber coupled with light stimulation but reduced exploration in chambers without light stimulation. Similar stimulation of the control ePet1-DRN^{mCherry} mice had no effects. (**H** and **I**) Changes in preference for the chamber conditioned (CS+) with VTA (H) or NAc (I) stimulation as well as that for the opposite chamber and the middle chamber. (**J**) A cell in the VTA of an ePet1-DRN^{ChR2} mouse was filled with 0.5% Neurobiotin in the recording pipette and labeled with Cy3-streptavidin. (**K**) The voltage traces of the cell shown in (J) in response to different current injections (-40 to 40 pA; 10 pA per step). (**L** and **M**) The morphology (green in L) and intrinsic properties of a cell in the NAc of *Vglut3*-/-;ePet1-DRN^{ChR2} mouse. Red in (L) indicates ChR2-mCherry^{+} fibers, and blue indicates DAPI counterstaining of cell nuclei. (**N**) VGluT3 immunoreactivity was present in the DRN of a *Vglut3*+/+ mouse, but not in that of *Vglut3*-/- mouse. Both mice were treated with colchicine.

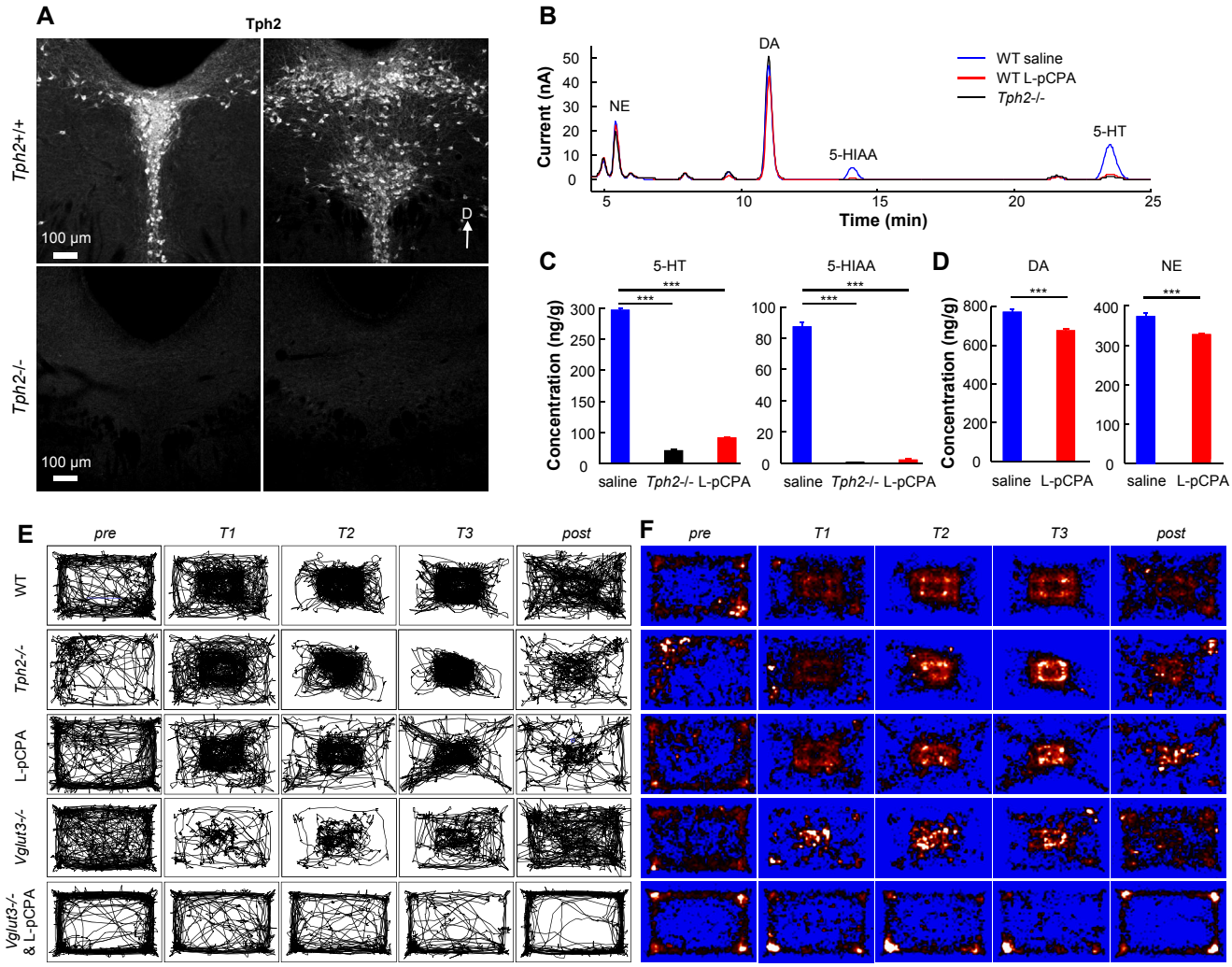

Figure S7. The effects of depleting 5-HT and knocking out *Vglut3* on the performance of iClass tests. Related to Figure 7. (**A**) Coronal sections of wild-type (upper panels) and *Tph2-/-* mice (lower panels) show that TPH2 knockout mice completely lack Tph2 expression. (**B**) HPLC-EC analysis of brain monoamine levels. (**C**) The levels of 5-HT in the whole brain of Tph2 KO mice and L-pCPA-treated mice were significantly reduced to 7% and 16% of control levels of saline-treated wild-type mice (left panel). The levels of 5-Hydroxyindoleacetic acid (5-HIAA), a key metabolite of 5-HT, were similarly reduced. ***, $p<0.001$; between-group t-tests. n =9 saline-treated mice, 10 *Tph2*-/- mice, and 10 L-pCPA-treated wild-type mice. (**D**) L-pCPA treatment slightly reduced brain dopamine and norepinephrine levels. ***, $p<0.001$; between-group t-tests; n = 10 mice for either group. (**E** and **F**) Locomotion tracks (E) and heat maps (F) show that knocking out the *Tph2* or *Vglut3* gene produced only mild phenotypes in iClass training. However, the reinforcement effect is completely eliminated following the disruption of 5-HT and glutamate release by injecting L-pCPA into *Vglut3*-/- mice. *Tph2*-/- and *Vglut3*-/- genotypes were based on ePet1-Cre background.

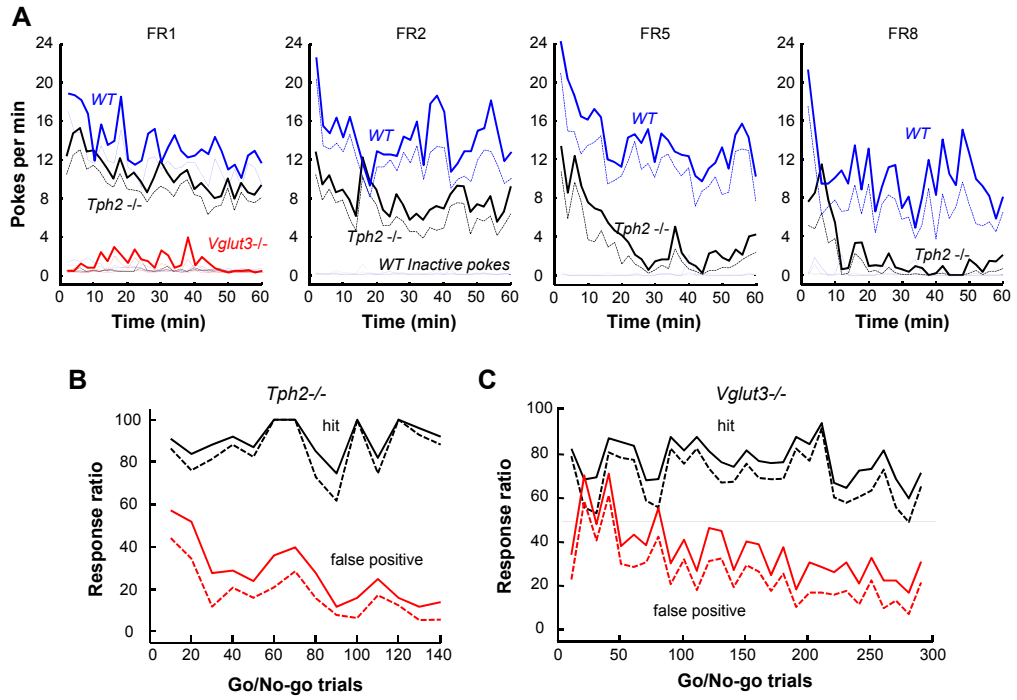

Figure S8. Tph2-/- and Vglut3-/- mutant mice exhibited a reduced performance in light self-stimulation tests and olfactory discrimination tests. Related to Figure 8. (**A**) The rates of poking rates across testing sessions with different schedules of fixed ratio (FR1, FR2, FR5, and FR8). Vglut3 but not Tph2 knockout mice had drastic reduction in the acquisition of self-stimulation with FR1 schedule. Tph2 knockout mice exhibited a much poorer performance with the schedules of FR5 and FR8. WT, *Tph2*-/- and *Vglut3*-/- genotypes were based on the ePet1-Cre background. (**B** and **C**) Hit and false positive response ratio throughout the Go/No-go training sessions for *Tph2*-/-; ePet1-DRN^{ChR2} mice (B) and *Vglut3*-/-;ePet1-DRN^{ChR2} mice (C).

Supplemental Movies (3 in total)

Supplementary Movie S1: **A video shows the exploratory behavior of an ePet1-DRN^{ChR2} mouse during the first 15-min long iClass training session (*T1*)**. Blue light pulses (15 ms, 20 Hz) were delivered through an optic fiber only when the mouse entered the marked center subarea. The mouse received its first stimulation at the time marked '0:00:30' and its second stimulation at '0:02:29'. The mouse was then quickly reinforced to explore the center area after a few more center entries. The video was compressed to play in a 5× fast forward mode and time tags are shown in the bottom left corner. Related to Figure 1.

Supplementary Movie S2: **The exploratory behavior during the second iClass training session (*T2*)**. The ePet1-DRN^{ChR2} mouse vigorously explored the center section throughout the 15-min training session. Related to Figure 1.

Supplementary Movie S3: Light stimulation of DRN Pet-1 neurons supported strong self-stimulation in an operant chamber. Nose poking of the active hole by the ePet1-DRN^{ChR2} mouse resulted in phasic stimulation (2s, 5 Hz) followed by a 5-s timeout period. The active hole was illuminated during the stimulation (2s) and timeout period (5s). Related to Figure 2.

Supplemental Experimental Procedures:

All procedures were conducted with the approval of the institutional Animal Care and Use Committee in accordance with governmental regulations of China.

Mice. The ePet1-Cre mouse line was produced by E.S. Deneris and colleagues (Case Western Reserve University) using the BAC-transgenic strategy (Jax Laboratory MGI allele Tg(Fev-cre)1Esd)(Scott et al., 2005). VGluT3 knockout (*Vglut3*-/-) mice were generated after replacing Exon 2 of the *Vglut3* gene in Chromosome 10 with an Frt-flanked neomycin resistance cassette (NEO) through homologous recombination in embryonic stem cells (129/Sv)(Gras et al., 2008). Tph2 knockout (*Tph2*-/-) mice were generated through the deletion of Exon 5, which encodes the tryptophan hydroxylase domain (Liu et al., 2011). To label all Pet-1 cells, we crossed the ePet1-Cre mouse line with the Ai14 reporter line (JAX strain 129S6-Gt(ROSA)26Sor <tm14(CAG-tdTomato)Hze>/J) to drive the expression of the red fluorescent protein tdTomato (ePet1-Cre;Ai14)(Madisen et al., 2009). Mice were maintained on a 12-h light/12-h dark cycle and housed in groups of five for 8 weeks. The mice were subsequently housed singly on a reverse light dark cycle (light off at 8AM) at least one week before behavioral experiments. Food and water were available *ad libitum*, except for water-deprived mice that underwent Go/No-go training using sucrose solution as the unconditioned reward.

AAV vectors and virus injection. The AAV-DIO-hChR2(H134R)-mCherry (simplified as AAV-DIO-ChR2-mCherry) construct was a gift of K. Deisseroth (Stanford University). In this construct, the gene encoding ChR2-mCherry fusion protein was cloned in the antisense direction and flanked by a pair of canonical loxP sites and a pair of mutated lox2272 sites (Atasoy et al., 2008). In the AAV-DIO-mCherry construct, the ChR2 sequence was removed from the AAV-DIO-ChR2-mCherry construct. Adeno-associated viral particles of serotype 9 for AAV-DIO-ChR2-mCherry and AAV-DIO-mCherry were produced at the Vector Core Facility at the University of Pennsylvania or in the laboratory of M. Luo (NIBS, Beijing) with the technical assistance of D. Duan (University of Missouri at Columbia). The final viral vector titers were in the range of 1-5 $\times 10^{12}$ particles/ml.

For virus injection into the DRN, the mice were anesthetized with pentobarbital (i.p., 80 mg/kg), mounted onto a mouse stereotaxic instrument and kept warm with an electric heating pad. A small hole in the skull was opened 3.8 mm posterior to bregma and 0.9 mm lateral to the midline. A guiding cannula (26 gauge, Plastics One) was implanted through the hole with a 15° angle from the lateral to medial and another 15° angle from the anterior to posterior (Figure S1A), and the tip of the internal cannula (33 gauge, Plastics One) was targeted at the central region of the DRN (DV=3.0 mm; Figure S1B). The virus was delivered through the internal cannula attached to a custom-made pressure injector. For each mouse, 1 μl of virus (AAV-DIO-ChR2-mCherry or AAV-DIO-mCherry) was injected into the DRN within 1 h. After viral injection, a dummy cannula replaced the internal cannula.

Behavioral tests.

intraCranial Light Administration in Specific Subarea (iClass). Individual mice were placed in an illuminated open field (41 × 29, L×W in cm) at 6 hrs after the start of the dark cycle. Within the open field, red lines marked a rectangular area (13 × 10.5, L×W in cm) as the target area for reinforcement (Figure 1D and Figure S2A, C). A mouse was allowed to freely explore the open field, and its movement was video recorded using an overhead infrared CCD camera at the rate of 25 fps.

The iClass task started 2-3 weeks after virus injection. The task consisted of three phases (pre-, training, and post/extinction) and each mouse took up to 8 days to complete the entire task. During the pre-phase on day 1 (*pre*), the basal locomotor activity of the mouse was recorded and measured in an open field. During the three training sessions in the following days (*T1-T3*), the mouse was lightly anaesthetized using isoflurane vapor, and an optical fiber was subsequently inserted into the DRN through the guiding cannula. After 2-min recovery, the mouse was gently placed in a corner of the open field, and its activity was monitored and calculated for 15 min. Whenever the centroid of the mouse body was located within the marked central rectangular area, blue light pulses, generated by a diode-pumped solid-state laser, were passed to the DRN through the optical fiber (473 nm wavelength, 15 ms pulse duration, 5 or 20 Hz frequency; 20 mW output power; fiber diameter = 200 μm and NA = 0.22). Light stimulation was immediately terminated when the centroid of the mouse body left the marked area. Animal

movement was recorded during the post-stimulation extinction sessions (*post1-post4*), but no light stimulation was applied.

After the behavior tests, the videos were analyzed offline using self-developed Matlab (MathWorks, MA, USA) computer programs. We quantified the following parameters for each animal: animal positions, travel distance, duration in the marked center area, and the number of entries to and exits from the center area. The experimental group consisted of ePet1-Cre mice injected with AAV-DIO-ChR2-mCherry virus into the DRN (simplified as ePet1-DRN^{ChR2}). In addition, iClass tests were performed on ePet1-DRN^{ChR2} mice lacking functional *Tph2* or *Vglut3* genes (*Tph2*-/-;ePet1-DRN^{ChR2} mice or *Vglut3*-/-;ePet1-DRN^{ChR2} mice, respectively). Wild-type littermates injected with AAV-DIO-ChR2-mCherry virus (WT-DRN^{ChR2}) or ePet1-Cre mice injected with AAV-DIO-mCherry virus (ePet1-DRN^{mCherry}) served as two different controls. The experimental and control groups underwent identical surgery and trainings. To chemically deplete 5-HT, ePet1-DRN^{ChR2} mice or *Vglut3*-/-;ePet1-DRN^{ChR2} mice were i.p. injected with L-pCPA (4-Chloro-L-phenylalanine hydrochloride, TCI,123053-23-6; in 0.1 M NaOH, pH=8) twice a day (9 am and 7 pm) at a dose of 100 mg/kg (calculated as freebase) for 3 consecutive days before being subjected to behavioral tests. L-pCPA injections were continued until the completion of behavior tests.

Self-stimulation in an operant chamber. Operant conditioning chambers (22×16×15, L×W×H in cm; AniLab Software and Instruments) were equipped with two nose-poke detectors (ENV-114M; Med Associates) located 2 cm above the metal grid floor and encased in sound-attenuating boxes. One nose poke detector was designated as 'active' and its activation triggered light delivery through an optical fiber to the DRN (473 nm wavelength, 15 ms pulse duration, 5 Hz for 2 s or 20 Hz for 3 s). Stimulation was followed by a 5 s timeout period. The hole associated with the 'active' detector was illuminated during the DRN stimulation time and the timeout period. Additional nose pokes during the illumination period had no programmed consequence. No outcome was associated with nose poking through the 'inactive' hole.

Following 2 weeks of post-surgical recovery, individual mice spent 1 h for context habituation and learned to emit operant responses. The mice were subsequently allowed to self-stimulate the DRN using the same

parameters with a fixed-ratio one (FR1) schedule for 1 h. During the following hours, the stimulation schedules were changed to FR2, FR5, and FR8, each of which lasted 1 h, with a 15-min rest period for food and water. Nose pokes of both active and inactive holes and the timing of stimulation were recorded using a computer.

Two-bottle preference test. The reward value of the DRN light stimulation was assessed through the two-bottle preference test as previously described (Domingos et al., 2011). The entire test lasted 6 days and two 2-h sessions were completed per day during the dark phase of animal activity. At the beginning of each day, a mouse was placed in a chamber (20 × 20× 22, L×W×H in cm) equipped with two contact lickometers connected to two bottles on opposite walls. The mouse contact of the lickometer was detected via a logic electronic circuit, which relayed digital 'lick' signals to a computer via parallel ports. On the first two days, both bottles were filled with water, and basal licking responses to the two water bottles were measured. The positions of the two bottles and their associated lickometers were swapped during the second session of each day. For light-stimulated ePet1-DRN^{ChR2} mice, the procedures within the next four days were largely similar to those during the first two days with the following exceptions. First, one of the bottles used in the first two days was assigned as a 'water' bottle, containing only water, coupled to laser stimulation upon animal licking of its nozzle. Second, the other bottle (assigned as 'sucrose') contained sucrose solution at the concentrations of 0, 1, 2, and 5%. Third, each sucrose concentration was used for one day, and the bottle positions were swapped during the two sessions of the day. The lick signals from the laser-coupled water bottle triggered light stimulation (473 nm, pulse duration 15 ms, 20 Hz for 1 s or 5 Hz for 2 s) to the DRN through an optical fiber. The light preference scores were calculated as the ratio of the number or duration of licks of the light-coupled water bottle to the total number or duration of licks during each session.

Go/No-go test. Olfactory Go/No-go learning was computer-controlled with custom-built electronic circuits and computer programs implemented with LABVIEW (National Instruments) (Hu et al., 2007). The mice were rewarded with either sucrose solution or light stimulation of the DRN. One group of mice consisting of wild-type littermates was rewarded with 5% sucrose solution. The test animals (ePet1-DRN^{ChR2}, *Tph2*-/-;ePet1-DRN^{ChR2}, *Vglut3*-/-;ePet1-DRN^{ChR2}, or *Vglut3*-/-;ePet1-DRN^{ChR2} mice injected with L-pCPA) were trained with DRN light

stimulation. All mice were deprived of water for 36 h prior to the shaping session. During the 'shaping' period, a mouse became familiarized with the Go/No-go chamber in the dark and was trained to locate and lick the drinking nozzle within the appropriate time window. The trials were started after the initial poking of the nose above the drinking nozzle to interrupt an infrared photo-beam. The drinking nozzle served as a contact lickometer and the lick signals were digitized using an electronic circuit and relayed to a computer. The animals learned to receive water by licking the nozzle at 0.2 s after the onset of 2 s-long blank air pulses, and the time window for action lasted 2 s. The 'shaping' process was terminated after 300 trials of training in a single day.

The mice were trained in three sequential phases: discrimination, switch, and reversal. During the discrimination phase, the mice learned to distinguish odor pulses containing n-amyl acetate or citral (1% saturated odor vapor for either odor). The mice licked the drinking nozzle to receive the reward of sucrose solution or DRN stimulation in response to n-amyl acetate (CS+; termed 'hit'). The licking response during citral (CS-) produced a mild penalty of 5 s timeout and the mice eventually learned to inhibit licking following CS- (termed 'correct rejection'). For nontransgenic littermates, licking after CS+ stimuli resulted in the opening of solenoid valve for the delivery of 5% sucrose solution. The drinking nozzle was closed for ePet1-DRN^{ChR2} mice, and thus licking within the time window of CS+ did not deliver the fluid reward. In contrast, an optical fiber was implanted above the DRN, and licking in response to CS+ resulted in light stimulation of the DRN consisting of blue light pulses (15 ms at 20 Hz for 3 s).

The mice trained with sucrose solution underwent 300 trials of training (150 trials of CS+ and CS-, respectively) each day and completed the 'discrimination' phase after 5 days (a total of 1500 trials). For ePet1-DRN^{ChR2} mice rewarded with DRN light stimulation, the entire discrimination phase consisted of 500 trials of training (250 trials of CS+ and CS- in pseudorandom order) within a single day. The *Tph2*-/-;ePet1-DRN^{ChR2} and *Vglut*3-/-;ePet1-DRN^{ChR2} mice could not complete 500 trials in a day and their discrimination phase was terminated after 6 h of training. A "correct ratio" was calculated after dividing the number of correct trials (hit and correct rejection) by the total number of trials in a training block of 50 (sucrose solution) or 10 trials (light stimulation).

After learning n-amyl acetate as CS+ and citral as CS- (A+/B-), both nontransgenic mice and ePet1-DRN^{ChR2} mice underwent the phase of 'switch' learning. At the beginning of this phase, the mice repeated 50-100 trials to discriminate n-amyl acetate and citral. The odorant pair was immediately replaced with a different pair of odorants (carvone as CS+ and ethanol as CS-; C+/D-) for the next 300 trials. The mice needed to learn to associate licking during the application of carvone with reward.

The 'reversal' learning represented the final phase of the task. The mice were initially presented with the pair of odorants that mice learned during the 'switch' phase: carvone as CS+ and ethanol as CS- (C+/D-). After 100 trials, the associated valences of the two odorants were immediately reversed, and the carvone became CS- and ethanol became CS+ (D+/C-). The reversal learning required 400 trials for animals trained with light stimulation and 600 trials for those trained with sucrose solution. The ePet1-DRN^{ChR2} mice typically abandoned any attempt of licking in response to odorants 100 trials after the onset of reversal training. For these animals, the reversal training was temporary suspended, and the animals repeated two or three trials of the 'reshaping' process in which sucrose solution and light pulses were simultaneously delivered following hit responses to the current CS+ stimulus. Only light stimulation was administered after the brief 'reshaping' process. The *Tph2*-/-;ePet1-DRN^{ChR2} and *Vglut3-/-*;ePet1-DRN^{ChR2} mice were not challenged with odor switch and odor reversal because their performance was not sufficiently stable even during the discrimination phase.

Conditioned place preference. A guide cannula (26 gauge, Plastics One) was unilaterally implanted into the VTA (AP -3.3 mm, ML 0.5 mm, DV 4.2 mm) or the caudal NAc medial shell (AP 1.05 mm, ML 0.5 mm, DV 3.2 mm) of ePet1-DRN^{ChR2} mice or ePet1-DRN^{mCherry} control mice. Following 3 weeks of post-surgical recovery, individual mice were then conducted to a CPP apparatus comprising two side chambers (26 × 23 × 26, L×W×H in cm) and a middle chamber (11.5 × 23 × 26). One side chamber had black walls and metal grill floor, and the other side chamber had white walls and a metal punched floor. The center chamber had plastic walls and a smooth metal floor. The mouse locomotion was tracked using a video system and analyzed offline. The entire CPP test consisted of 3 phases: preconditioning phase on day 1, conditioning phase on days 2 and 3, and test phase on day 4. During the preconditioning phase, individual mice were allowed to freely explore the entire apparatus for 15

min. Any mouse that exhibited a strong initial preference for one of the side chambers (greater than 2 min difference) was excluded from further experiments. During the conditioning phase, mice were first confined to one side chamber for 20 min. Trains of blue light pulses (20 Hz, 15 ms, 20 s on/10 s off) were passed into the VTA or NAc. Four hours later, the mice were confined to the opposite side for 20 min with optic fiber inserted, but no light pulses were delivered. Each mouse was conditioned in the same side chamber, but the two side chambers were evenly conditioned for the entire test group. During the test phase, the mice were allowed to freely explore the entire apparatus for 15 min. The proportion of the 15-min sessions spent in each chamber was recorded. The results were compared with the proportion of time spent in that chamber in preconditioning sessions.

For terminal stimulation in the VTA and NAc, we also microinjected lidocaine into the DRN to prevent the potential antidromic activation of cell bodies. In addition to the guiding cannula for optical fiber, a 26-gauge guiding cannula (Plastics One) was implanted above DRN. Immediately before iClass training or CPP conditioning, lidocaine (20 μg in 1 μl of PBS; Sigma) was infused into the DRN through a 33-gauge internal cannula (25 μl/min; Plastics One). The internal cannula remained in place for an additional 2 min before being replaced by a dummy and an optical fiber was then inserted into the VTA or NAc for light stimulation.

Physiological recordings from brain slices. AAV-DIO-ChR2-mCherry virus was injected into the DRN of ePet1-Cre mice (ePet1-DRN^{ChR2} or *Vglut3*-/-;ePet1-DRN^{ChR2} mice; 8-12 weeks old, either sex). After 3 weeks of recovery, the mice were deeply anesthetized with pentobarbital (100 mg/kg i.p.) and intracardially perfused with ~5 ml ice-cold oxygenated modified artificial cerebrospinal fluid (aCSF) at a rate of ~2 ml/min. The modified aCSF for perfusion contained (in mM): 225 sucrose, 119 NaCl, 2.5 KCl, 0.1 $CaCl_2$, 4.9 $MgCl_2$, 1.0 NaH_2PO_4, 26.2 $NaHCO_3$, 1.25 glucose, 3 kynurenic acid, and 1 Na L-ascorbate (all chemicals for brain slicing were from Sigma-Aldrich). After perfusion, the brain was quickly removed and placed in ice-cold oxygenated aCSF containing (in mM): 110 choline chloride, 2.5 KCL, 0.5 $CaCl_2$, 7 $MgCl_2$, 1.3 NaH_2PO_4, 25 $NaHCO_3$, 20 glucose, 1.3 Na ascorbate, and 0.6 Na pyruvate. Coronal or horizontal sections (300 μm thick) were prepared using a Leica VT1200S vibratome. The slices were incubated for 1 h at 34 °C with aCSF saturated with 95% O_2/5% CO_2 and containing (in mM) 125 NaCl,

2.5 KCl, 2 $CaCl_2$, 1.3 $MgCl_2$, 1.3 NaH_2PO_4, 25 $NaHCO_3$, 10 glucose, 1.3 Na ascorbate, and 0.6 Na pyruvate. Before recording, a slice was transferred to a chamber on an Olympus BX51WI upright fluorescent microscope. The slices were submerged and superfused (2 ml/min) with aCSF at 28 °C.

$ChR2^+$ neurons in the DRN were recognized based on the expression of mCherry fluorescence in somata. Neurons within the VTA or NAc shell were identified through DIC microscopy, and the presence of ChR2-mCherry+ axonal terminals within the surrounding area was confirmed through fluorescence microscopy. The internal solution within whole-cell recording pipettes (4-7 MΩ) contained (in mM): 130 K-gluconate, 10 HEPES, 0.6 EGTA, 5 KCl, 3 Na_2ATP, 0.3 Na_3GTP, 4 $MgCl_2$, and 10 Na_2phosphocreatine (pH 7.2–7.4). Voltage-clamp and current-clamp recordings were performed using a MultiClamp700B amplifier (Molecular Devices). For voltage-clamp recordings, the neurons were held at -60 mV. Traces were low-pass filtered at 2.6 kHz and digitized at 10 kHz (DigiData 1440, Molecular Devices). The data were acquired and analyzed using Clampfit 10.0 software (Molecular Devices). For light stimulation, the tip of an optical fiber (200 μm core diameter, NA = 0.22) coupled to a 473-nm laser was submerged in aCSF and placed ~300 μm from the recording site. The delivery of light pulses (5 ms, 0.2-20 mW/mm^2) was controlled through digital commands from the Digidata 1440. For drug application, DNQX (10 μM, Sigma), picrotoxin (50 μM, Sigma) and ketanserin (10 μM, Sigma) were added to the superfusion medium through the dilution of stock solutions. The $GABA_A$ receptor antagonist picrotoxin was constantly perfused to isolate glutamatergic currents.

Electrophysiological recordings from behaving mice.

Recording from the DRN during olfactory discrimination. Individual mice were anesthetized with pentobarbital (80 mg/kg, i.p.) for surgery. A craniotomy was made for virus injection (1 μl of AAV-DIO-ChR2-mCherry) and the placement of an optetrode. A custom-made head-plate was subsequently affixed on the skull of ePet1-DRN^{ChR2} mice with stainless steel screws and dental cement. The mice were allowed to recover in individual cages for 2-3 weeks. Before training, the mice were water-deprived for 36 hrs and head-fixed onto two horizontal bars above a spherical treadmill supported by floating air (Zhan and Luo, 2010). The mice were trained to discriminate two odorants with the Go/No-go paradigm. A click sound was provided at 2 s before odorant

pulses to indicate trial onset. Air pulses containing citral or n-amyl acetate (1% saturated vapor, 1 s, 2 L/min) were presented in pseudorandom orders with the inter-trial interval of at least 12 s. Citral (CS+) was associated with a 2-s response time window at 1 s after the odorant pulse. Licking during this time window resulted in the delivery of 5% sucrose solution. N-amyl acetate (CS-) was not paired with any outcome. The drinking nozzle was placed near the tongue of the head-fixed mouse and an infrared laser beam was used to detect lick signals. Correct responses consisted of trials in which mice licked during the time window after citral ('hit') and inhibited licking during the time window after n-amyl acetate ('correct rejection'). The mice were trained for 2 days to achieve a stable performance >90% correct.

After training, we conducted recordings from the DRN of head-fixed mice during the performance of olfactory discrimination tasks on the same spherical treadmill. Extracellular spiking signals were recorded with custom-made 16-channel optetrodes comprising 4 tetrodes and an optical fiber (100 μm dia). The tetrodes were wound from 12.7 μm Ni-Cr-Fe wires (Stablohm 675; California Fine Wire, CA, USA) and gold-plated to reduce impedance to 250-500 KΩ. An optical fiber was glued to the tetrodes with epoxy and the fiber tip was placed ~500 μm above the ends of tetrodes. Optetrodes were lowered into the DRN with a micromanipulator (MP285; Sutter Instrument, CA, USA). Extracellular signals were recorded by a custom-made 16-channel amplifier with built-in bandpass filters (0.5-3.6 kHz). One channel, which did not show action potentials, was selected as a virtual reference to minimize moving artifact. Analog signals were digitalized at 25 kHz and collected using a Power1401 digitizer and Spike2 software (CED, Cambridge, UK). Before and after the task, trains of blue light pulses (5 ms duration, 10 Hz, ~5 mW) were applied to verify neuron types. Light intensity was adjusted to reduce spike jitter. After recordings, we generated electrolytic lesions with DC current injection through two electrodes (15–20 s; 100 μA) to verify the recording sites.

Single units were sorted offline using a Spike2 program for tetrode recordings. A single unit was positively identified as being Pet-1^+ if light pulses reliably (>50% vs. ~2.5% chance level) evoked spikes of similar waveforms (≥0.85 Pearson's correlation coefficient between evoked spikes and spontaneous spikes) within the 5 ms light pulses (overall latency = 3.9 ± 0.1 ms; n=60 cells). Physiological traces were aligned based on odor onset,

with the trial initiation signal at -1.5 s. We calculated the receiver operating characteristic (ROC) value of the neural activity throughout each trial by comparing the spike firing rates in a test window of 200 ms (100 ms advance step) aligned with respect to the firing rates in a control window at 2 s before the signal of trial onset (Nakamura et al., 2008). ROC values of CS+ trials and CS- trials were separately treated as ROC(CS+, control) and ROC(CS-, control). We also computed the ROC(CS+, CS-) to contrast the neural firing of CS+ trials to CS- trials in the same test window. We used ROC[CS+(epoch), CS-(epoch)] as a selectivity index to probe the neural response selectivity to reward-associated tasks in a certain epoch (immediately after task onset (-1.5 – -0.5 s), odor pulses (0 – 1 s), delay (1 – 2 s), licking/no-licking time window(2 – 4 s)). An ROC value of 1 indicates complete selectivity for reward tasks, while 0 indicates selectivity for non-reward tasks. The response strength was calculated as the ROC value comparing the neural activity in one of the epochs to the baseline level. To determine significance of neuronal response strength and selectivity, we performed permutation tests by using 1000 bootstrap replicates and $p < 0.01$ was considered statistically significant (Ranade and Mainen, 2009).

Recording from the M1 cortical area during a brain-machine interface task. An optical fiber was inserted above the DRN through the implanted cannula after the injection of 1 μl AAV-DIO-ChR2-mCherry. Custom-made head-plates were placed on the skulls, and the mice were allowed to recover for 2-3 weeks after surgery. On the day of recording, a small craniotomy was made above the vibrissa primary motor cortex (vM1; AP=1.3 mm, ML=0.7 mm). The dura matter was carefully removed, and four tetrodes were lowered ~500 μm below the cortical surface.

Spike waveforms that exhibited the highest S/N ratio were sorted online using a Spike2 program for tetrode recordings. Overall firing rates from 2-5 well-isolated single cells were binned (500 ms per bin) and engaged into a custom-written program in Spike2 in combination with a custom-written program developed in LABVIEW. The delivery of odorant pulses (10 s) was triggered if the ensemble firing rates were below a threshold (threshold-1) that was set based on initial baseline firing rate. A train of blue light pulses (473 nm; 15 ms duration, 20 Hz, 3 s) were delivered into the DRN once the ensemble firing rates crossed a higher threshold (threshold-2) during the presence of the odor. The value of threshold-2 was above the value of mean + 2*SEM of basal firing rate during

the 5-s pre-stimulus period. Using this value, threshold crossing occurred during 10-20% trials of odorant application before training with light stimulation. When two odors were used during discrimination test, only one odor was coupled with laser stimulation. Threshold crossing during another odor resulted in mild air puff toward one of animal eyes. The events of threshold crossing were sent from the Spike2 program to the LABVIEW program, which generated timing signals to a customized electronic circuit to control odorant delivery, light stimulation, and air puff. For omission tests, no light was given even when the firing rates of the well-trained ensembles were above the preset threshold-2. The contingency degradation was implemented by delivering light stimulation at a random point outside of the time window for odorant pulse. The contingency between the neural activity and laser stimulation was reinstated after 40-100 trials of omission or degradation.

After recordings, signals were further sorted offline with Spike2 and then analyzed using custom-written programs in the Matlab. The percentage of crossing the pre-determined threshold-2 was calculated as correct ratio in a bin of 500 ms. Neuronal response strength was determined by calculating ROC values of the ensemble firing during the first 3 s (0 – 3 s) of odorant application in comparison to a control period (-5 to -3). The learning curve was plotted as the change of neural response strength along training trials. Permutation tests were used to detect whether the response strength was statistically significant ($p < 0.01$).The learning curve was plotted as neural response strength changing along training trials.

Histology and immunohistochemistry. Mice were killed with an overdose of pentobarbital and perfused intracardially with 0.1 M phosphate buffer saline and then 4% paraformaldehyde. After cryoprotection in 30% sucrose, coronal sections (35 μm thickness) were cut on a cryostat (Leica CM1900) and used for immunohistochemical examination using standard histochemical methods. Briefly, the sections were blocked with 3% BSA or 10% normal goat serum in PBS with 0.3% Triton X-100 and subsequently incubated with primary rabbit antibodies against 5-HT (1:4000, Sigma; 20 hrs), Tph2 (1:400, Millipore; 20 hrs), VGluT3 (1:1000, Synaptic Systems; 48 hrs), TH (1:500, Invitrogen; 20 hrs) at 4°C. The signals were visualized with Cy2-conjugated secondary antibodies (1:200, Jackson ImmunoResearch). The sections were cover-slipped with 50% glycerol and DAPI in the mounting medium. To elevate VGluT3 protein signals in somata, both wild-type and *Vglut3*-/- mice

were treated with an intracerebroventricular injection of colchicine (6 μg within 1 μl) at 48 h before perfusion fixation.

Fluorescent signals were acquired using a Zeiss LSM510 Meta confocal microscope. The optical sectioning thickness was ~2 μm, and the stack of images for a specific brain section was projected onto a single image for presentation. The spatial spread and labeling accuracy of ChR2-mCherry or mCherry were examined based on the presence of red mCherry fluorescence in Tph2+ DRN neurons.

Measurement of brain monoamine levels. Brain monoamines were measured using high performance liquid chromatography coupled with electrochemical detection (HPLC-EC). Whole brains of adult male mice (L-pCPA group & saline control) were dissected on ice. Brains were weighed immediately to milligram and extracted with a buffer containing $HClO_4$ (0.94 M), EDTA-Na_2 (0.5 mM) and L-Cysteine (0.83mM). Each milligram of brain tissue corresponded to the volume of 2 μl extraction buffer volume. The homogenates were centrifuged at 4 ℃ (12,000 rpm for 30 min). Supernatants or standard samples (50 μl) were injected to separate HPLC columns. The mobile phase consisted of NaCl (3 mM), EDTA-Na_2 (0.2 mM), CH_3COONa (100 mM), octanesulfonic acid sodium (0.9 mM) and citric acid monohydrate (85 mM; pH3.7). The flow rate was 1 ml/min. Data was analyzed using CoulArray software (ESA) based on standard samples.

Supplemental References

Atasoy, D., Aponte, Y., Su, H.H., and Sternson, S.M. (2008). A FLEX switch targets Channelrhodopsin-2 to multiple cell types for imaging and long-range circuit mapping. J Neurosci *28*, 7025-7030.

Domingos, A.I., Vaynshteyn, J., Voss, H.U., Ren, X., Gradinaru, V., Zang, F., Deisseroth, K., de Araujo, I.E., and Friedman, J. (2011). Leptin regulates the reward value of nutrient. Nat Neurosci *14*, 1562-1568.

Gras, C., Amilhon, B., Lepicard, E.M., Poirel, O., Vinatier, J., Herbin, M., Dumas, S., Tzavara, E.T., Wade, M.R., Nomikos, G.G.*, et al.* (2008). The vesicular glutamate transporter VGLUT3 synergizes striatal acetylcholine tone. Nat Neurosci *11*, 292-300.

Hu, J., Zhong, C., Ding, C., Chi, Q., Walz, A., Mombaerts, P., Matsunami, H., and Luo, M. (2007). Detection of near-atmospheric concentrations of CO2 by an olfactory subsystem in the mouse. Science *317*, 953-957.

Liu, Y., Jiang, Y., Si, Y., Kim, J.Y., Chen, Z.F., and Rao, Y. (2011). Molecular regulation of sexual preference revealed by genetic studies of 5-HT in the brains of male mice. Nature *472*, 95-99.

Madisen, L., Zwingman, T.A., Sunkin, S.M., Oh, S.W., Zariwala, H.A., Gu, H., Ng, L.L., Palmiter, R.D., Hawrylycz, M.J., Jones, A.R.*, et al.* (2009). A robust and high-throughput Cre reporting and characterization system for the whole mouse brain. Nat Neurosci *13*, 133-140.

Nakamura, K., Matsumoto, M., and Hikosaka, O. (2008). Reward-dependent modulation of neuronal activity in the primate dorsal raphe nucleus. J Neurosci *28*, 5331-5343.

Ranade, S.P., and Mainen, Z.F. (2009). Transient firing of dorsal raphe neurons encodes diverse and specific sensory, motor, and reward events. J Neurophysiol *102*, 3026-3037.

Ren, J., Qin, C., Hu, F., Tan, J., Qiu, L., Zhao, S., Feng, G., and Luo, M. (2011). Habenula "cholinergic" neurons co-release glutamate and acetylcholine and activate postsynaptic neurons via distinct transmission modes. Neuron *69*, 445-452.

Scott, M.M., Wylie, C.J., Lerch, J.K., Murphy, R., Lobur, K., Herlitze, S., Jiang, W., Conlon, R.A., Strowbridge, B.W., and Deneris, E.S. (2005). A genetic approach to access serotonin neurons for in vivo and in vitro studies. Proc Natl Acad Sci USA *102*, 16472-16477.

Zhan, C., and Luo, M. (2010). Diverse patterns of odor representation by neurons in the anterior piriform cortex of awake mice. J Neurosci *30*, 16662-16672.